

Understanding of tuning techniques of converter controllers for VSC-HVDC

Chandra Bajracharya, Marta Molinas, *Member IEEE*, Jon Are Suul, Tore M Undeland, *Fellow IEEE*

Abstract— A mathematical model of a voltage source converter is presented in the synchronous reference frame for investigating VSC-HVDC for transferring wind power through a long distance. This model is used to analyze voltage and current control loops for the VSC and study their dynamics. Vector control is used for decoupled control of active and reactive power and the transfer functions are derived for the control loops. In investigating the operating conditions for HVDC systems, the tuning of controllers is one of the critical stages of the design of control loops. Three tuning techniques are discussed in the paper and analytical expressions are derived for calculating the parameters of the current and voltage controllers. The tuning criteria are discussed and simulations are used to test the performance of such tuning techniques.

Index Terms—Voltage source converter; VSC-HVDC; Vector control; PI controller tuning; modulus optimum; symmetric optimum

I. INTRODUCTION

NORTH of Norway has extremely good conditions for establishment of wind power generation farms, with a possibility of about 4000MW of wind power generation in this area. The main grid in Northern Norway consists of a weak 132 kV network, and considering the integration of massive amounts of wind power, the existing transmission lines, will not be able to handle and export the surplus energy from these areas to the consumption areas in the middle of Norway. Alternative methods are being considered for the integration of this new energy into the existing system. One of the alternatives is to build a new corridor with multi-terminal HVDC from Northern Norway to Middle of Norway. VSC-HVDC, the HVDC technology based on voltage source converters (VSC), has recently been an area of growing interest due to a number of factors: its modularity, independence of ac network, independent control of active and reactive power, low power operation and ability of power reversal etc [1]. VSC-HVDC technology has been promoted under the commercial trade names HVDC Light [2] and HVDC Plus (the “plus” stands for Power Link Universal Systems) [3]-[4] by two prominent manufacturers.

C. Bajracharya is with Norwegian University of Science and Technology, O.S. Bragstads plass 2E, 7491 Trondheim, Norway (47-7359-4237; fax: 47-7359-4279; e-mail: chandrb@stud.ntnu.no).

M. Molinas, J. A. Suul and T. Undeland are with Norwegian University of Science and technology (e-mail: marta.molinas@elkraft.ntnu.no, jon.are.suul@elkraft.ntnu.no, tore.undeland@elkraft.ntnu.no).

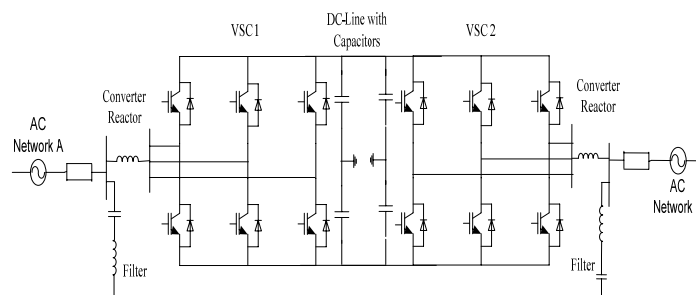


Fig. 1. VSC based HVDC link

As shown in Fig.1, a VSC based HVDC link consists of VSCs connected back to back via a dc-link. For analysis of the complete VSC-HVDC system, this paper starts from developing an understanding of a VSC from the control point of view. The control strategy used is based on field oriented vector control [5] of voltage source current controlled converters.

The VSC-HVDC operating characteristics are determined by the controllers including the system. Adequate performance of VSC-HVDC system under diverse operating conditions depends on the selection of robust parameters for the control system. Usually, due to the simple structure and robustness, PI controllers have been used to adjust the system for desired responses. The tuning of the converter controller parameters (gain and time constant) is a compromise between speed of response and stability for small disturbances as well as the robustness to tolerate large signal disturbances. Furthermore, the control loops are nonlinear in nature, and hence needs careful selection of control parameters to accommodate a range of operating conditions. Tuning rules should also take into account the effects of non-ideal operating conditions and try to minimise them.

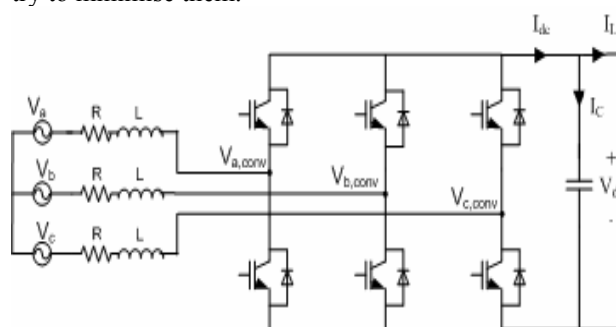


Fig. 2. Three phase PWM-VSC connected to ac source

In addition to the effects of controller tuning on the performance of the VSC-HVDC, it is claimed in [6] that design of converter control systems has an impact on sub-synchronous torque interaction. There exists certain parameter region of the converter controllers where unstable shaft torsional oscillations between the VSC-HVDC transmission link and a nearby generator may be caused. It is also claimed that with proper control parameter settings, no sub-synchronous damping control is needed.

This paper focuses on the control structure and tuning of the voltage source converter. The decoupled control of real and reactive power exchanged between the converter and the electric power system is explained. Analytical expressions, transfer functions and the tuning rules for the PI controllers are presented and discussed in an attempt to establish the criteria for tuning.

II. SYSTEM DESCRIPTION

Fig.2 shows a schematic diagram of an ac source/grid connected to a PWM-voltage source inverter. The control of the converter aims at regulating the dc voltage V_{dc} and maintaining the balance between the dc link power and ac power supply. For that, standard field oriented vector control technique is implemented which gives decoupled control of active and reactive power [7].

For the analysis of the system, basic equations describing the system behavior are presented based on analysis done in [8]-[10]. The phase voltages and currents are given by the equation ,

$$V_{abc} = R \cdot i_{abc} + L \frac{d}{dt} i_{abc} + V_{abc,conv} \quad (1)$$

where V_{abc} , i_{abc} , $V_{abc,conv}$ are ac voltages, currents and converter input voltages respectively and R and L resistance and filter inductance between the converter and the ac system.

The converter 3-phase currents and voltages are expressed in 2-axis d-q reference frame, synchronously rotating at given ac frequency, ω . The voltage equations in d-q synchronous reference frame are,

$$L \frac{d i_d}{d t} = - R \cdot i_d + \omega L \cdot i_q - V_{dc,conv} + V_d \quad (2)$$

$$L \frac{d i_q}{d t} = - R \cdot i_q - \omega L \cdot i_d - V_{q,conv} + V_q$$

The power balance relationship between the ac input and dc output is given as,

$$p = \frac{3}{2} (v_d \cdot i_d + v_q \cdot i_q) = v_{dc} \cdot i_{dc} \quad (3)$$

where v_{dc} and i_{dc} are dc output voltage and current respectively. On the output side,

$$i_{dc} = C \cdot \frac{d v_{dc}}{d t} + i_L \quad (4)$$

The d-axis of the rotating reference frame (Park's) is aligned to the ac voltage vector so that $v_q = 0$. With this alignment, the instantaneous real and reactive power injected into or absorbed from ac system is given by,

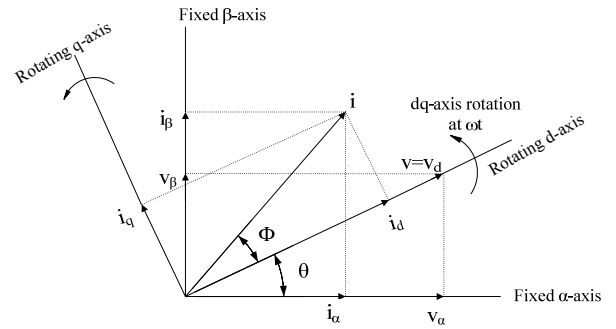


Fig. 3. Transformation of axes (α - β to d-q) for vector control

$$p = \frac{3}{2} \cdot v_d \cdot i_d \quad (5)$$

$$q = \frac{3}{2} \cdot v_d \cdot i_q$$

Therefore, the control of active and reactive power reduces to the control of d and q components of current. The angular position of the voltage vector is given by,

$$\theta = \tan^{-1} \left(\frac{v_\beta}{v_\alpha} \right) \quad (6)$$

where v_α and v_β are components of voltage in stationary two axis reference frame (Clark's). The angle θ is computed using a phase lock loop (PLL) technique [11]-[12].

III. PRESENTATION OF THE CONTROL SCHEME

The control scheme for the three-phase voltage source inverter is considered as cascade of two independent controllers, a dc voltage controller providing reference signals to the control system and the current controller that generates the switching signals according to the reference and measured signals, as shown in Fig 4.

A. Current Controller

As the currents are transformed to the synchronous reference frame, they become dc signals under balanced sinusoidal conditions and perfect synchronization [13]. Then PI controllers will ensure zero steady state error and increased robustness of the closed loop system.

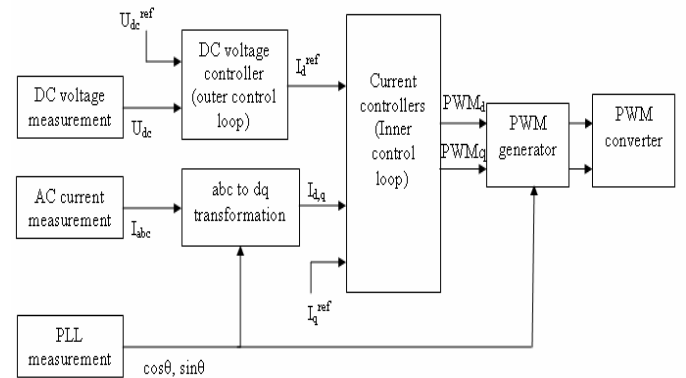


Fig. 4. Functional control diagram of VSC using vector control

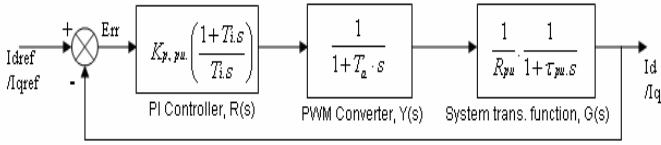


Fig. 5. Block diagram of PI Current control scheme in per unit

The control system requires a decoupled control of i_d and i_q . However, the model in synchronous frame (2) shows that the two axes are coupled due to the cross terms $\omega L \cdot i_q$ and $\omega L \cdot i_d$. When the cross coupling terms are compensated by feed-forward, the d-axis and q-axis components of currents can be controlled independently. Synchronous reference frame PI regulators then regulate the d and q components of currents. The two independent control loops in per unit system can be obtained [14] to be as shown in Fig. 5, where $K_{p,pu}$ and T_i are PI controller parameters, T_a is the delay caused by VSC switches and τ_{pu} is the per unit time constant of the line.

B. DC-link Voltage Controller

The current controller as described earlier ensures that the output current tracks the reference values generated by an additional external control loop, which performs the output active power regulation by implementing control of dc voltage. From (3)-(5), the dc link dynamics is given by,

$$C \cdot \frac{dV_{dc}}{dt} = \frac{3}{2} \cdot \frac{V_d}{V_{dc}} \cdot I_d - I_L \quad (7)$$

The minimum value of required dc side voltage [15] is given by the inverter output voltage as,

$$V_{dc} = 2 \cdot \sqrt{\frac{2}{3}} \cdot V_{LL,rms} = 2 \cdot V_{peak,ph} \quad (8)$$

where $V_{peak,ph}$ is peak phase voltage at the ac side and $V_{LL,rms}$ is the line-line rms voltage.

The dc-link dynamics, (7) is a non-linear equation and the parameters for the PI regulator need to be selected using linearization of system model around the operating point. The reference point for linearization is found by specifying reference input ($V_{dc,ref}$) for the nonlinear model. The linearization yields the transfer function as [14],

$$\frac{\Delta V_{dc}(s)}{\Delta i_d(s)} = \frac{3}{2} \cdot \frac{V_{d,0}}{V_{dc,ref}} \cdot \frac{1}{s \cdot C} \quad (9)$$

For the analysis of the outer dc voltage control loop, the second order closed loop transfer function of the inner current controller is approximated by equivalent first order transfer function by equating the error functions of two transfer functions, which gives the equivalent time constant, T_{eq} to be $2T_a$ [14].

C. Feedforward in DC-link controller

Although simple to design and implement, a cascade control system is likely to respond to changes more slowly than a control system where all the system variables are processed and acted upon simultaneously [16]. The feed-forward is used to minimize disadvantage of slow dynamic response of cascade control.

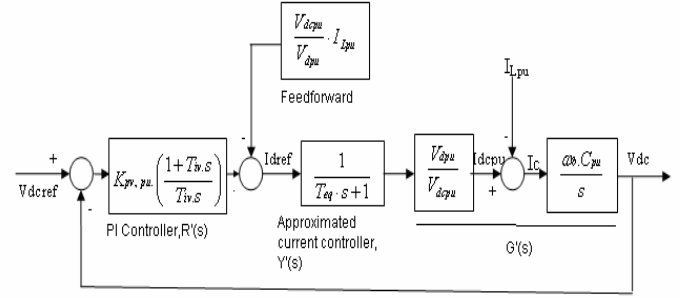


Fig. 6. Block diagram of dc-link voltage control scheme in pu

Using feed-forward, the load variation can be greatly reduced and the large gain of voltage controller otherwise required to reduce the large error is not necessary, which is important from stability viewpoint.

The dc link voltage controller controls the capacitor current so as to maintain the power balance. Hence under balanced conditions, $i_c = 0$. That is, $I_{dc} = I_L$.

Thus, the reference value of I_d should be,

$$I_d = \frac{2}{3} \cdot \frac{V_{dc}}{V_d} \cdot I_L \quad (10)$$

which is the feed-forward term, ensuring exact compensation for load variation.

When the system equations are analysed in per unit [14], the complete block diagram of dc-link voltage controller can be represented as in Fig.6, where $K_{p,pu}$ and T_{iv} are PI controller parameters, T_{eq} is the equivalent time constant of first order approximation of current control loop, and C_{pu} is per unit capacitance of dc link.

IV. TUNING OF PI CONTROLLERS

In the tuning process of PI controllers, the nonlinearities are generally neglected, and tuning is done following the criteria adopted for electric drives [17]. Cascade control requires the speed of response to increase towards the inner loop. Hence, internal loop is designed to achieve fast response. On the other hand, main goal of outer loop are optimum regulation and stability. The inner loop is tuned according to ‘‘modulus optimum’’ condition because of fast response and simplicity whereas the outer loop according to ‘‘symmetrical optimum’’ condition for optimizing system behavior with respect to disturbance signals [18].

A. Modulus Optimum

For low order controlled plants without time delay the modulus optimum (absolute value optimum criterion) is often used in the conventional analog controller tuning. When the controlled system has one dominant time constant and other minor time constant, the standard form of the control system transfer function for the modulus optimum is achieved by cancelling the largest time constant, while the closed loop gain should be larger than unity for as high frequencies as possible [19]. This method is widely used because of its simplicity and fast response.

The open loop transfer function of current controller is given as,

$$G_{C,OL}(s) = K_{p,pu} \cdot \left(\frac{1+T_i \cdot s}{T_i \cdot s} \right) \cdot \frac{1}{1+T_a \cdot s} \cdot \frac{1}{R_{pu}} \cdot \frac{1}{1+s \cdot \tau_{pu}} \quad (11)$$

The modulus optimum tuning criteria for this system gives the PI controller parameters as,

$$T_i = \tau_{pu} \quad (12)$$

$$K_{p,pu} = \frac{\tau_{pu} \cdot R_{pu}}{2 \cdot T_a} \quad (13)$$

This tuning criterion gives the open loop and closed loop transfer functions of the current control loop as follows.

$$G_{C,OL}(s) = \frac{1}{2 \cdot T_a} \cdot \frac{1}{s \cdot (1+T_a \cdot s)} \quad (14)$$

$$G_{C,CL}(s) = \frac{1}{2T_a^2 s^2 + 2T_a s + 1} \quad (15)$$

The resulting system has a frequency of natural oscillation $\omega_n = 1/T_a \sqrt{2}$ and damping factor $\zeta = 1/\sqrt{2}$. Because this method is based on simplification by pole cancellation, and optimizing the absolute value to 1, the resulting response of the system would always correspond to values of ζ and ω_n as above. The system can however, be tuned for a desired value of crossover frequency by choosing total constant gain term of (11) to be equal to the desired crossover frequency. The crossover frequency of current open loop is chosen one or two order smaller than switching frequency of converter to avoid interference from switching frequency noise.

B. Symmetrical Optimum

When the controlled system has one dominant time constant and other minor time constant, the PI controller can be tuned using the modulus optimum criteria as described in previous section. However, when one of the poles is already near to the origin or at the origin itself, the pole shift does not change the situation significantly. The open loop transfer function of the voltage controller already has two poles at the origin. An alternative criterion to tune the controllers in this condition is given by the symmetrical optimum criteria.

A symmetrical optimum design criterion obtains a controller that forces the frequency response of the system as close as possible to that for low frequencies. The method has the advantage of maximizing the phase margin. As phase margin is maximized for given frequency, the system can tolerate more delays, which is important for systems having delays. This method optimizes the control system behaviour with respect to disturbance input. The method has well established tuning rules and has good disturbance rejection [20]. An extended approach of tuning by symmetric optimum [21] is presented here.

From the system block diagram as developed in Fig. 5, the open loop transfer function of the system without considering the feed-forward and the disturbance input is given by,

$$G_{V,OL}(s) = K_{pv,pu} \cdot \left(\frac{1+T_{iv} \cdot s}{T_{iv} \cdot s} \right) \cdot \frac{1}{1+T_{eq} \cdot s} \cdot \left(\frac{V_{dpu}}{V_{dcpu}} \cdot \frac{\omega_b \cdot C_{pu}}{s} \right) \quad (16)$$

For given open loop transfer function of the system, cancellation of pole by setting $T_{iv} = T_{eq}$ is impossible as it leads to two poles at origin and the system becomes unstable.

Introducing $K = \frac{V_{dpu}}{V_{dcpu}}$ and $T_c = 1/\omega_b \cdot C_{pu}$, the transfer

function can be written as,

$$G_{V,OL}(s) = K_{pv,pu} \cdot \left(\frac{1+T_{iv} \cdot s}{T_{iv} \cdot s} \right) \cdot \frac{K}{1+T_{eq} \cdot s} \cdot \left(\frac{1}{s \cdot T_c} \right) \quad (17)$$

The tuning criteria according to symmetrical optimum is obtained using the Nyquist criteria [22] of stability,

$$|G_{V,OL}(j\omega)| = 1, \text{ and } \angle G_{V,OL}(j\omega) = -180^\circ + \Phi_M \quad (18)$$

where Φ_M is the phase margin. Differentiation of the angle criteria with respect to ω gives the condition for maximum value of phase margin, which is,

$$\omega_d = \frac{1}{\sqrt{T_{iv} \cdot T_{eq}}} \quad (19)$$

This condition gives the tuning criteria for time constant of the controller as,

$$T_{iv} = T_{eq} \cdot \left(\frac{1 + \sin \Phi_M}{1 - \sin \Phi_M} \right) \quad (21)$$

The resulting open loop frequency characteristic will have a maximum phase Φ_M at the crossover frequency of ω_d , symmetric about $1/T_i$ and $1/T_{eq}$. Then by symmetric property, we can also write,

$$T_{iv} = a^2 \cdot T_{eq} \quad (22)$$

where 'a' is the symmetrical distance between $1/T_{iv}$ to ω_d , and $1/T_{eq}$ to ω_d . Then from the magnitude condition, the tuning for gain of controller can be found as follows.

$$K_{pv,pu} = \frac{T_c}{K \cdot \sqrt{T_{iv} \cdot T_{eq}}} = \frac{T_c}{a \cdot K \cdot T_{eq}} \quad (23)$$

Now using the PI controller parameters, the open loop transfer function and the closed loop transfer function become,

$$G_{V,OL}(s) = \frac{1}{a^3 \cdot T_{eq}^2 \cdot s^2} \cdot \left(\frac{1 + a^2 \cdot T_{eq} \cdot s}{1 + T_{eq} \cdot s} \right) \quad (24)$$

$$G_{V,CL}(s) = \frac{1 + a^2 \cdot T_{eq} \cdot s}{1 + a^2 \cdot T_{eq} \cdot s + a^3 \cdot T_{eq}^2 \cdot s^2 + a^3 \cdot T_{eq}^3 \cdot s^3} \quad (25)$$

As it is seen that the denominator of the closed loop transfer function has a pole, $s = -1/a \cdot T_{eq}$. Hence, the system can be simplified as follows.

$$G_{V,CL}(s) = \frac{1 + a^2 \cdot T_{eq} \cdot s}{(a \cdot T_{eq} \cdot s + 1) \cdot (a^2 \cdot T_{eq}^2 \cdot s^2 + a \cdot (a-1) \cdot T_{eq} \cdot s + 1)} \quad (26)$$

Most of the literature use $T_{iv} = 4T_{eq}$ ($a=2$) for the optimization according to conventional symmetrical optimum tuning [21]. The resulting performance gives an overshoot of around 43%, settling time around $16.3 T_{eq}$ and a phase margin of about 36° . The phase margin value is low and the system has a high overshoot, but still the system response is fast. It is possible to compensate the overshoot and enhance the performance of controller by employing a filter in the reference signal. Another option is to choose a higher value of a , so that the phase margin is increased and the damping is also improved, but then, the system response becomes slower. Hence the choice of the controller parameters from design point of view is a compromise between the performances. The recommended

value of the ratio T_{iv}/T_{eq} is constrained between 4 and 16 in literature [23].

From the denominator of the transfer function (26), the eigenvalues to the characteristic equations are,

$$s_1 = \frac{-1}{a.T_{eq}} \quad (27)$$

$$s_2, s_3 = -\left(\frac{a-1}{2.T_{eq}}\right) \pm \sqrt{\left(\frac{a-1}{2.a.T_{eq}}\right)^2 - \left(\frac{1}{a.T_{eq}}\right)^2} \quad (28)$$

This generalization shows three conditions for roots s_2, s_3 :

- $a < 3$, the roots are complex conjugate.
- $a = 3$, roots are real and equal
- $a > 3$, roots are real and distinct.

Thus for a given value of T_{eq} , if 'a' is varied, the roots start from complex conjugate roots on imaginary axis for $a=1$, and move away from imaginary axis, becoming real and equal at $a=3$ and if increased further, the roots move along the real axis. The damping factor can be changed by varying 'a'. So the value of 'a' can be chosen for the condition fulfilling desired performance. The specifications could be the cross-over frequency at which the phase margin is maximum, or the value of desired phase margin. However, the specifications should result in the value of 'a' in the acceptable region.

There are no explicit specification of performance indicators like damping factor or settling time, and it is difficult to analytically express these performances in terms of 'a', as the closed loop system is a third order system. However, for closed loop system (26), if the real pole is located very far from the origin, transients corresponding to such remote pole are small, last for short time and can be neglected. The system can then be approximated by a second order system, for an easier estimate of response characteristics. But when specifying 'a', there is no control over relative spacing of the real pole and the complex poles, so such a simplification and degree of freedom can not be achieved.

C. Pole placement interpretation of Symmetric Optimum

Using the symmetric optimum method, controllers can be tuned for variable damping by specifying the value of a , but the range of variation is very small. Lower values of 'a' give a small phase margin and high oscillations, while increasing values of 'a' may lead to better damping but slower response. Symmetrical optimum method can be extended so as to specify damping factor for the system as part of tuning procedure using pole placement [23].

This method considers the special case when $a < 3$, that is the characteristic equation has one real root, p and a pair of complex conjugate root, $\sigma \pm j\omega$. Then it results in a characteristic equation,

$$s^3 + (p+2\sigma).s^2 + (2p\sigma + \sigma^2 + \omega^2).s + p.(\sigma^2 + \omega^2) \quad (29)$$

The real pole placement is defined through a relation,

$$p = \alpha . \sigma \text{ where } \alpha > 1.$$

and for the complex roots, the relation between damping factor and the roots is defined as

$$\omega^2 = \frac{1 - \zeta^2}{\zeta^2} . \sigma^2 \quad (30)$$

Then, the characteristic equation is,

$$s^3 + (\alpha + 2).\sigma.s^2 + \left(2\alpha + 1 + \frac{1 - \zeta^2}{\zeta^2}\right).\sigma^2.s + \left(1 + \frac{1 - \zeta^2}{\zeta^2}\right).\sigma^3 \quad (31)$$

But the characteristic equation of the system (17) is,

$$s^3 + \frac{1}{T_{eq}}.s^2 + \frac{K_p.K}{T_c.T_{eq}}.s + \frac{K_p.K}{T_i.T_c.T_{eq}} \quad (32)$$

Equating the coefficients of (31) and (32), the controller parameters can be found in terms of α and ζ . And, specifying ζ for calculating controller parameters has more explicit physical meaning than specifying 'a' as in previous case.

V. APPLICATION OF TUNING RELATIONS

Considering the system given in [7], with system parameters $L_{pu} = 0.15$, $C_{pu} = 0.88$, $R_{pu} = 0.01$ and $\omega_b = 377$, the cases of parameter tuning of the controller are presented using the tuning rules of modulus optimum, symmetric optimum and explicit damping factor specification. The switching frequency of the converter block (f_{switch}) is taken as 10kHz. Average time delay of converter is then

$$T_a = \frac{T_{switch}}{2} = \frac{1}{2.f_{switch}} \quad (33)$$

A. Tuning of current controller using modulus optimum

The current controller was tuned using modulus optimum criteria.

Controller gain, $K_{p,pu} = 3.9788$

Integral time constant, $T_i = 0.039788$

The open loop transfer function as shown in Fig. 7 had a phase margin of 65.5° and gain margin infinity showing the closed loop system to be stable.

The time response to step input was studied, which gave the results as in Fig. 8.

Maximum Overshoot, $M = 1.042$

Time for maximum overshoot, $t_m = 0.0003s$

Settling time, using 2% criteria, $t_s = 0.0004s$

The open loop bode plot gives the open loop crossover frequency of 9.1×10^3 rad/s (1.448 kHz), which is about 7 times smaller than the switching frequency of 10 kHz, indicating acceptable ratio [16].

B. Tuning of voltage controller using symmetric optimum

For the steady state operating conditions, $V_{dpu} = V_{dcpu} = 1pu$, and choosing $a = 3$, the controller parameters are tuned according to symmetrical optimum condition.

Controller gain, $K_{pv,pu} = 10.0474$

Integral time constant, $T_{iv} = 0.0009$

The bode plot of open loop transfer function in Fig.9 shows stable operating limits with a maximum phase margin of 53.1° , occurring at the crossover frequency of 3.33×10^3 rad/s (530.5Hz).

The step response of the system is shown in Fig.10 which has following characteristics:

Maximum Overshoot, $M = 1.25$

Time for maximum overshoot, $t_m = 0.0009s$

Settling time, using 2% criteria, $t_s = 0.0024s$

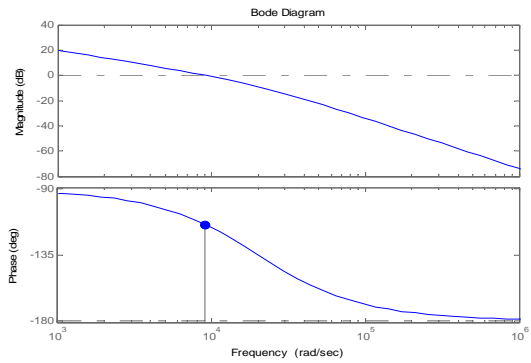


Fig. 7. Open loop Bode plot of current controller transfer function

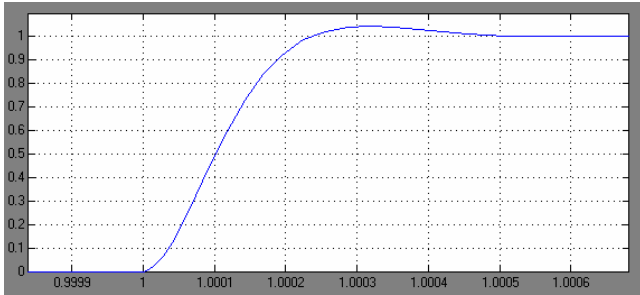


Fig. 8. Step response of Current controller tuned with modulus optimum

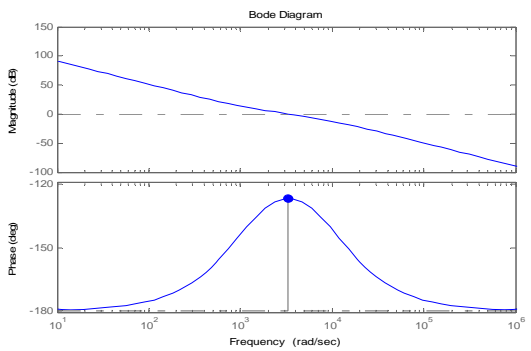


Fig. 9. Open loop Bode plot of voltage controller transfer function tuned with symmetric optimum

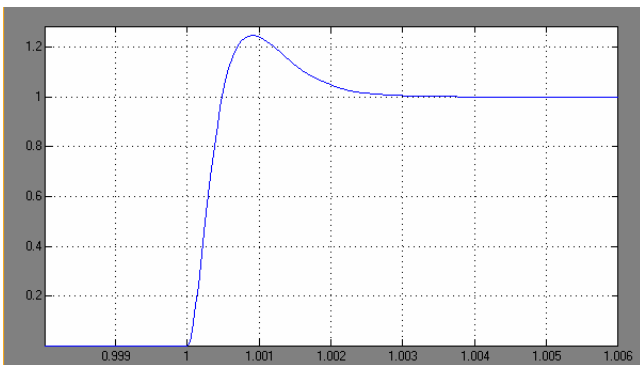


Fig. 10. Step response of Voltage controller tuned with symmetric optimum

C. Tuning of voltage controller using pole placement of symmetric optimum

Tuning voltage controller using pole placement is just a special case of tuning using symmetric optimum, where the

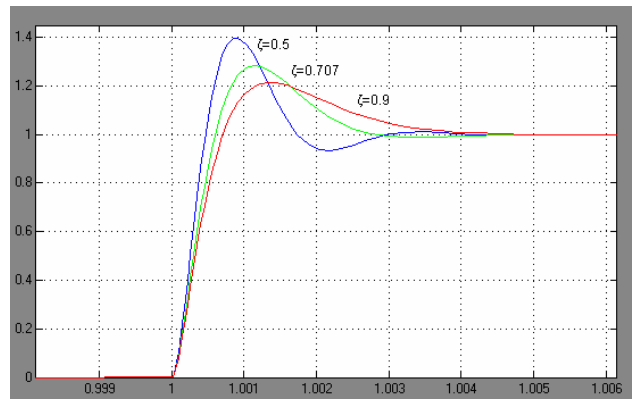


Fig. 11. Step response for fixed value of $\alpha=5$, and varying $\zeta = 0.5, 0.707$ and 0.9

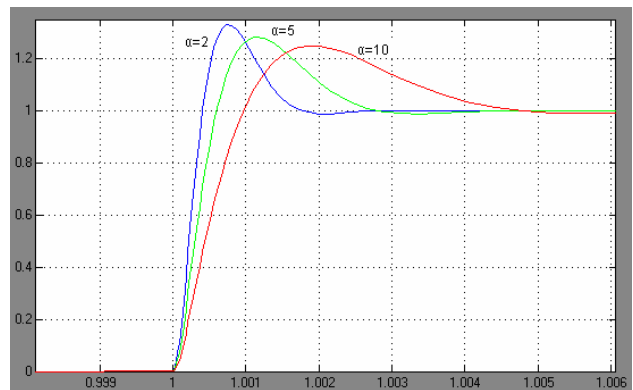


Fig. 12. Step response for fixed value of $\zeta=0.707$, and varying $\alpha = 2, 5$ and 10

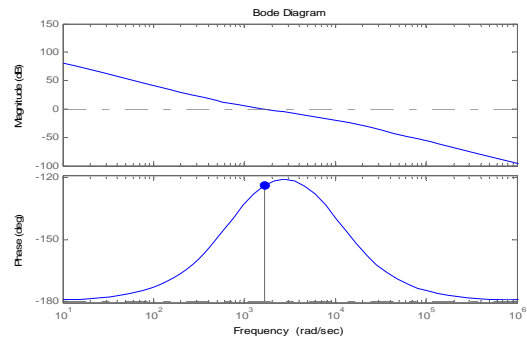


Fig. 13. Open loop Bode plot of voltage controller transfer function when tuned with pole placement

placement of the real pole and the damping of complex pole can be specified. There are two parameters α and ζ that can be specified for a desired performance and the variation of step response with these parameters are shown in Fig. 11 and 12. It is seen that by specifying the damping factor of the complex poles, the overshoot in the step response of third order system can be changed. With increasing ζ , the overshoot is decreased and the speed of response is slightly decreased. On the other hand, for a given value of ζ increase in α seems to make the response slow with slight decrease in overshoot.

For a particular case of $\alpha=10$ and $\zeta=0.707$, the controller parameters were tuned by pole placement resulting in, Controller gain, $K_{pv, pu} = 4.6052$

Integral time constant, $T_{iv} = 0.0013196$

The open loop bode plot of the system in Fig.13 shows a stable operation with phase margin 56° at crossover frequency of 1.66×10^3 rad/s (264.19Hz).

The time domain response of the system to step input has the following response:

Maximum Overshoot, $M = 1.25$

Time for maximum overshoot, $t_m = 0.0019s$

Settling time, using 2% criteria, $t_s = 0.0043s$

As compared to symmetric optimum, the tuning of controllers using pole placement method results in a slower response. But still the speed of response is acceptable. In this method by specifying α and ζ the closed loop poles of the system are configured. However, as it is a special case when the closed loop system has a pair of complex poles, there is not much freedom in choosing the pole-zero configurations. The advantage of this method might be stated as the explicit specification of damping ratio and pole-zero configurations, that has better implications than specification of parameter ' α ' in normal case.

VI. DISCUSSION OF TUNING CRITERIA

Adjustment of current controller according to modulus optimum provides good response with small overshoot to a step change of reference. Because of the cancellation of slow process pole by the controller zero, the response is considerably improved. If set point responses are predominant factor of concern, pole-zero cancellation might be right, but if load responses or disturbance rejection are also important, this method may not be sufficient [24]. The cancellation controller has good set point response but leads to a very slow disturbance response, because system poles are not altered in the disturbance transfer function, resulting controller zero to become poles in disturbance transfer function [25]. In addition to that, an inexact cancellation also results in sluggish response and poor robustness. Moreover, if the time constant of the input system (τ) is large, the integral time constant of the controller will increase. This will also cause the capability of controller for disturbance rejection to become poor. These factors need to be considered in further applications.

Adjustment of voltage controller according to symmetric optimum provides high proportional gain and low integral time constant, which results in fast response as well as strong rejection of disturbance. With this method of tuning, substantial overshoot can be seen in the step response, which might require limiting of rate of change of voltage reference. Moreover, additional filtering might also be required for ripple in dc bus voltage. But again, the additional filtering will decrease the controller gain and the bandwidth. Modification of symmetric optimum using pole placement is possible for the special case where the closed loop system has complex poles. Explicit specification of damping factor for complex poles can be used to specify the closed loop pole-zero configuration and set the response of the system. But as seen from Fig. 13, the resulting system is not the optimum one from the phase margin point of view.

Both of the tuning criteria, modulus optimum and symmetric optimum are based on optimisation of dynamic performance of the controlled system. However, in tuning of

PI controllers for HVDC, only considering the dynamic performance is not sufficient.

The control design is based on the assumption that the inner and outer loops are decoupled and hence, can be linearized. Non ideal operating condition leads to generation of harmonics, influencing both ac and dc control. When low order harmonics are present in the system, the two control loops cannot be considered decoupled. The current loop is designed considering constant dc bus voltage because the voltage control loop is much slower than the inner current control loop. If dc voltage has low frequency ripple, it cannot be considered constant for current loop design.

In order to investigate the possible problems to be encountered in VSC-HVDC installation, detailed analysis of dynamic behaviour of the system and development of suitable controllers to overcome the problems are needed. The tuning rules of the controllers should be devised to reduce negative influence on system performance due to non-ideal operating conditions, system non-linearities etc.

VII. CONCLUSIONS

A mathematical model of a three phase VSC in synchronous reference frame was presented, and based on the model, current and voltage control of VSC was studied. The tuning methods were investigated for PI controller parameter setting. Method of modulus optimum was used to derive parameters of current regulators, and symmetrical optimum to derive parameters of voltage controller. Some possible problems in tuning were presented and discussed, which will be studied further through simulation to derive general guidelines for tuning controllers for improved performances.

VIII. FURTHER WORK

A good understanding of control strategies, and control system, their drawbacks and advantages in most general operating conditions, is necessary to derive the most relevant option for control. In further work, analysis of control system and controller tuning will be continued. With the development of the control platform, the controllers will be tested under several circuit conditions, to test the capability and robustness of the controller to handle the adverse situations. The simulation platform will be built in PSCAD to study the control system under different conditions of load disturbances, unbalance conditions etc. with different tuning rules. The simulation results would be studied for verification of operating range, and for severe disturbances to test control robustness. Effect of nonlinearities and unbalanced voltage conditions will also be studied through simulations. This work will be directed to the establishment of general guidelines for tuning the controllers and suggestions for improving the controller performances.

APPENDIX

A. Park and Clark transformation system

Transformation	Transforms	Matrix for transformation
Clark transformation	from abc to $\alpha\beta$	$\frac{2}{3} \begin{pmatrix} 1 & -1/2 & -1/2 \\ 0 & \sqrt{3}/2 & -\sqrt{3}/2 \end{pmatrix}$
Inverse Clark transformation	from $\alpha\beta$ to abc	$\begin{pmatrix} 1 & 0 \\ -1/2 & \sqrt{3}/2 \\ -1/2 & -\sqrt{3}/2 \end{pmatrix}$
Park transformation	from $\alpha\beta$ to dq	$\begin{pmatrix} \cos \theta & \sin \theta \\ -\sin \theta & \cos \theta \end{pmatrix}$
Inverse Park transformation	from dq to $\alpha\beta$	$\begin{pmatrix} \cos \theta & -\sin \theta \\ \sin \theta & \cos \theta \end{pmatrix}$

B. Base values for Per Unit System

The following base system is chosen for conversion of the system into Per Unit (p.u.) representation.

S_b = Nominal three-phase power of the ac-grid

V_b = Nominal peak phase voltage at the ac side [$V_{peak,ph}$]

$$= \sqrt{\frac{2}{3}} V_{LL,rms} \text{ where } V_{LL,rms} = \text{Line-Line RMS Voltage}$$

$$I_b = \text{Nominal peak phase current} = \frac{2}{3} \cdot \frac{S_b}{V_b}$$

$$Z_b = \text{Base ac impedance} = \frac{V_b}{I_b}$$

ω_b = Base frequency

The base for per unit transformation is chosen as to achieve a power invariant transformation, so that the ac and dc side power is the same.

As, $S_{3\text{phase}} = 3 \cdot V_{\text{phase}} \cdot I_{\text{phase}}$ and then the power balance gives,

$$S_b = \frac{3}{2} \cdot V_b \cdot I_b = V_{dcbase} \cdot I_{dcbase}$$

The base value for dc voltage is chosen as,

$$V_{dcbase} = 2 \cdot V_{\text{peak,ph}} = 2 \cdot V_b,$$

Then by the power balance equation as above,

$$I_{dcbase} = \frac{3}{4} \cdot I_b$$

$$\text{And, } Z_{dcbase} = \text{Base dc impedance} = \frac{V_{dcbase}}{I_{dcbase}} = \frac{8}{3} \cdot Z_b$$

REFERENCES

[1] ABB publication, "Its Time to Connect", <http://www.abb.com/cawp/gad02181/c1256d71001e0037c1256893005121c7.aspx>

[2] Costa Papadopoulos et al, "Interconnection of Greek islands with dispersed generation via HVDC Light technology", ABB

[3] http://www.siemens.com/page/1.3771.1007570-1-12_0_0-0.00.html

[4] F.Schettler, H.Huang and N.Christl, "HVDC transmission systems using voltage sourced converters - design and applications", *IEEE Summer Power Meeting*, July 2000, Vol.2, pp 715-720.

[5] De Donker, R. W. and Novotny, D. W., "Universal Field Oriented Controller", *IEEEIAS Annual Conference Record*, Pittsburgh, 1988, pp. 450-456.

[6] Kohachiro Nishi, Tatsuhito Nakajima and Akihiko Yokoyama, "Steady-state stability of shaft torsional oscillation in ac-dc interconnected system with self-commutated converters", *Scripta Technica, Electr Eng Jpn*, 128(4), 25-37, 1999.

[7] C.Schauder, H. Mehta, "Vector Analysis and Control of Advanced Static Var Compensators", *IEE Proceedings-C*, Vol.140, No.4, July 1993.

[8] Marta Molinas, Bjarne Naess, William Gullvik, Tore Undeland, "Robust Wind Turbine system against Voltage sag with induction generators interfaced to the grid by power electronic converters", *IEEJ Trans. IA*, Vol 126, No 7, 2006.

[9] R Pena, J C Clare, G M Asher, "Doubly fed induction generator using back to back PWM converters and its application to variable speed wind energy generation", *IEE Proc.-ElectrPower Appl.*, Vol 143, No 3, May 1996.

[10] Ruihua Song et al, "VSC based HVDC and its control strategy", *IEEE/PES Trans. and Distrib. Conference and Exhibition*, 2005.

[11] J. Svensson, "Synchronisation methods for grid-connected voltage source converters," *Proc. Inst. Electr. Eng.-Gener. Transm. Distrib.*, vol. 148, no. 3, pp. 229-235, May 2001.

[12] S.-K. Chung, "Phase-locked loop for grid-connected three-phase power conversion systems," *Proc. Inst. Electr. Eng-Electron. Power Appl.*, vol.147, no. 3, pp. 213-219, May 2000.

[13] F. N. Gakis, S. A. Papathanassiou, "Simple control schemes for grid-connected three-phase voltage-source inverters of DG units", *Proc.XVII International Conference on Electrical Machines, ICEM'2006*, 2-5Sept.2006 Chania, Greece.

[14] Chandra Bajracharya, "Control of VSC-HVDC for wind power", Specialization project, NTNU, Jan. 2008.

[15] Ned Mohan, Tore M. Undeland and W. P. Robbins, *Power Electronics: Converters, Applications and Design*, John Wiley and Sons Inc.

[16] Ned Mohan, *Electric Drives: An Integrative Approach*, MNPERE, 2003, pp8-18.

[17] M. Liserre, "Innovative control techniques of power converters for industrial automation", PhD Thesis, Politecnico di Bari, Italy, Dec. 2001.

[18] W. Leonhard, *Introduction to Control Engineering and Linear control Systems*, New Delhi, 1976.

[19] Á. J. J. Rezek, C. A. D. Coelho, J. M. E. Vicente, J. A. Cortez, P. R. Laurentino, "The Modulus Optimum (MO) Method Applied to Voltage Regulation Systems: Modeling, Tuning and Implementation", *Proc. International Conference on Power System Transients, IPST'01*, 24-28 June 2001, Rio de Janeiro, Brazil.

[20] O. Aydin, A. Akdag, P. Stefanutti, N. Hugo, "Optimum Controller Design for a Multilevel AC-DC Converter System", *Proc. Of Twentieth Annual IEEE Applied Power Electronics Conference and Exposition, APEC 2005*, 6-10 March 2005, Vol. 3, pp. 1660-1666

[21] S. Preitl, R.-E. Precup, "An Extension of Tuning Relations after symmetrical Optimum Method for PI and PID Controllers", *Automatica*, Vol. 35, 1999, pp 1731-1736.

[22] K. Ogata, *Modern Control Engineering*, Prentice Hall International.

[23] M. Machaba, M. Braae, "Explicit Damping Factor Specification in Symmetrical Optimum Tuning of PI Controllers", *Proc. of First African Control Conference*, 3-5 Des. Cape Town, South Africa, pp. 399-404.

[24] C. C. Hang, "The Choice of Controller Zeros," *IEEE Control Systems Magazine*, Vol. 9, No. 1, Jan. 1989, pp.72-75

[25] R. N. Clark, "Another Reason to Eschew Pole-Zero Cancellation," *IEEE Control Systems Magazine*, Vol.8, No. 2, April 1988, pp. 87-88.